medRxiv preprint doi: https://doi.org/10.1101/2020.04.09.20060053; this version posted April 15, 2020. The copyright holder for this preprint (which was not certified by peer review) is the author/funder, who has granted medRxiv a license to display the preprint in perpetuity. It is made available under a CC-BY-NC-ND 4.0 International license .

COVID-19 pandemics modeling with SEIR(+CAQH), social distancing, and age stratification. The effect of vertical confinement and release in Brazil.

Wladimir Lyra[1,*], José-Dias do Nascimento Jr.[2,3], Jaber Belkhiria[4,5], Leandro de Almeida [2], Pedro Paulo M. Chrispim[6,7], Ion de Andrade[8,9],

1 Department of Astronomy, New Mexico State University, PO Box 30001, MSC 4500, Las Cruces, NM 88003-8001, USA; wlyra@nmsu.edu
2 Dep. de Física Teórica e Experimental, Universidade Federal do Rio Grande do Norte, Avenida Senador Salgado Filho, 3000. 59078-970. Natal/RN, Brazil.
3 Harvard-Smithsonian Center for Astrophysics, Cambridge, MA 02138, USA
4 One Health Institute, School of Veterinary Medicine, University of California, Davis, CA, USA.
5 Center for Animal Disease Modeling and Surveillance, Department of Medicine & Epidemiology, School of Veterinary Medicine, University of California Davis, CA, USA.
6 Instituto Alicerce Ensino Pesquisa e Inovação em Saúde, R Cinco De Julho, 176/101, Rio De Janeiro, RJ, CEP 22051030, Brazil
7 Hospital do Coração, Laboratório de Implementação do Conhecimento em Saúde, R Desembargador Eliseu Guilherme, 147, Paraíso SP, 04004-030, Brazil
8 Secretaria de Estado da Saúde Pública/SESAP/Cefope - Escola Técnica do SUS - ETSUS, Av. Alexandrino de Alencar, 1850, Tirol, Natal, RN, Brazil
9 Laboratório de Inovação Tecnológica em Saúde, Av. Nilo Peçanha, 620 - 59012-300 Petrópolis - Natal/RN - Brazil

Abstract

The ongoing COVID-19 epidemics poses a particular challenge to low and middle income countries, making some of them consider the strategy of "vertical confinement". In this strategy, contact is reduced only to specific groups (like age groups) that are at increased risk of severe disease following SARS-CoV-2 infection. We aim to assess the feasibility of this scenario as an exit strategy for the current lockdown in terms of its ability to keep the number of cases under the health care system capacity. We developed a modified SEIR model, including confinement, asymptomatic transmission, quarantine and hospitalization. The population is subdivided into 9 age groups, resulting in a system of 72 coupled nonlinear differential equations. The rate of transmission is dynamic and derived from the observed delayed fatality rate; the parameters of the epidemics are derived with a Markov chain Monte Carlo algorithm. We used Brazil as an example of middle income country, but the results are easily generalizable to other countries considering a similar strategy. We find that starting from 60% horizontal confinement, an exit strategy on May 1st of confinement of individuals older than 60 years old and full release of the younger population results in 400 000 hospitalizations, 50 000 ICU cases, and 120 000 deaths in the 50-60 years old age group alone. The health care system avoids collapse if the 50-60 years old are also confined, but our model assumes an idealized lockdown where the confined are perfectly insulated from contamination, so our numbers are a conservative lower bound. Our results discourage confinement by age as an exit strategy.

NOTE: This preprint reports new research that has not been certified by peer review and should not be used to guide clinical practice.

medRxiv preprint doi: https://doi.org/10.1101/2020.04.09.20060053; this version posted April 15, 2020. The copyright holder for this preprint (which was not certified by peer review) is the author/funder, who has granted medRxiv a license to display the preprint in perpetuity. It is made available under a CC-BY-NC-ND 4.0 International license .

Introduction

The severe acute respiratory syndrome coronavirus 2 (SARS-CoV-2) outbreak has been ongoing for 5 months now [1]. Since it was first reported in Dec 2019 in China [2], the virus rapidly made its way to other parts of the world taking pandemic proportions[3]. The number of cases and deaths exponentially incremented reaching a total of 1.5 million confirmed cases and 88 thousand deaths in early April 2020. Recent diseases outbreaks that spilled over from animals such as Ebola [4, 5] or Avian Influenza [6] have been described as specific to developing countries. COVID-19 has been breaking this myth as the virus has been particularly exceptional at breaching in inside all developing countries and challenging their health system. In Europe, Italy has been particularly affected. With 140 thousand cases, the Italian national health system's has been struggling to effectively respond to the exponentially increasing flow of patients in need for intensive care [7]. The United States recently surpassed China in total number of cases (420 thousand), becoming a particular hot bed in this phase of the pandemics [8]. By the time this article is published, there will not be a place on earth where the virus did not cause any damage. West African countries such as Sierra Leone just reported their first cases [9] and catastrophic scenario similar to the 2016 Ebola outbreak is possible.

The threats of COVID-19 on countries that started to count cases prompted us to develop a model to describe the evolution of the epidemic and its effects the health care system. Mathematical models are a powerful tool that proved their importance in previous epidemiological disasters such as the Ebola virus [10, 11], smallpox [12], or influenza [13], contributing to the understanding of the dynamics of disease and providing useful predictions about the potential transmission of a disease and the effectiveness of possible control measures, which can provide valuable information for public health policy makers [14]. SIR-type models, also known as Kermack-McKendrick model [15], consists of a set of differential equations and has been applied to a variety of infectious diseases. Although considered as simple, SIR models have been of great help to stop epidemics in the past such as putting in place effective vaccination protocols [16].

Here we develop an SIR type compartmental models for COVID-19 including both symptomatic and asymptomatic, quarantined, and hospitalized while taking into consideration differences by age groups. We also analysed at the effect of confinement during a specific period of time. Contrary to similar epidemiological models, the proposed SIR model is initiated by the first confirmed COVID-19 death. Numerical simulations of the deterministic models are compared with real numbers of the ongoing outbreak in different countries. Moreover, the deterministic framework in which we operate greatly simplifies model analysis and allows a more thorough comparison of the various intervention strategies.

We focus on this paper on the case of Brazil, where the pandemics counts 16 000 confirmed and cases and 800 fatalities at the time of writing. The country has 35 682 ICU beds according to government data of Feb 2020 [17]. The first official SARS-CoV-2 case in Brazil was reported in in São Paulo on February 26th and the first official SARS-CoV-2 case was confirmed on March 19th. Shortly after, a lockdown was enacted first in Rio de Janeiro on March 22nd, then on other regional urban centers. There are no clear estimate on the percentage population that is actually in confinement. However, it is estimated to be around is 56% according to satellite data [1],

Given socio-economic consequences of a lockdown, particularly on a middle income country, decision makers are considering a *vertical confinement* as an exit strategy to the regular lockdown. Vertical confinement is understood as reducing contact to a specific age group that is more at risk of contracting and developing SARS-CoV-2 [18],

[1] `https://bit.ly/2URlQcK`

medRxiv preprint doi: https://doi.org/10.1101/2020.04.09.20060053; this version posted April 15, 2020. The copyright holder for this preprint (which was not certified by peer review) is the author/funder, who has granted medRxiv a license to display the preprint in perpetuity. It is made available under a CC-BY-NC-ND 4.0 International license .

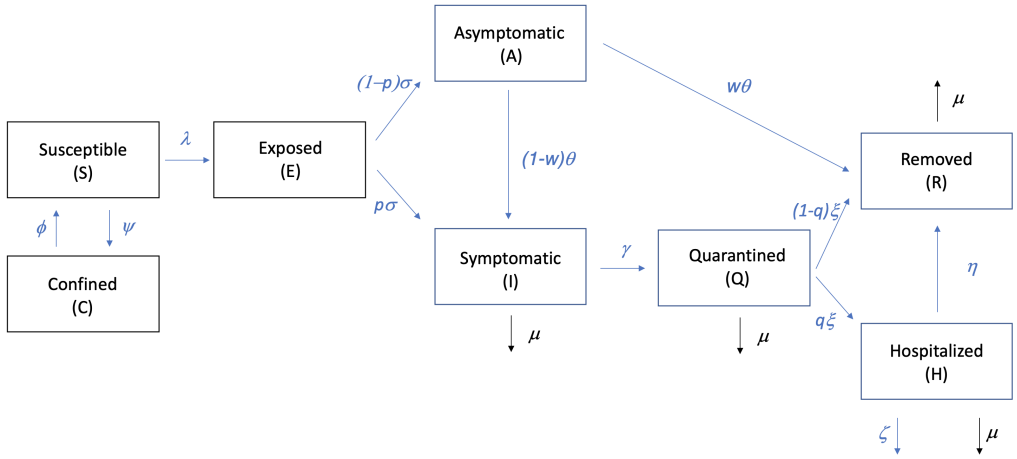

Fig 1. Schematic flow chart between compartments.

as opposed to *horizontal* (or general) confinement that does not discriminate between age groups. Throughout this manuscript, we will present the model which we validated with data on other countries. We then applied the model to the specific SARS-CoV-2 scenario in Brazil. We finally tested the effect of both general confinement and the vertical one on the epidemic curve.

Needs a global conclusion on application of the model to other low middle income countries and how this could help decision makers make efficient decisions to stop causalities.

The model

We used a modified version of an SIR-type deterministic compartmental model to trace COVID-19 epidemic evolution in an isolated population of N individuals[2]. We assumed that a population could be subdivided into the following compartments:

- Susceptible (S): COVID-19 naive individuals,
- Confined (C): subset of susceptibles removed from the epidemics (by e.g. social distancing).
- Exposed (E): Susceptible that have been exposed to infective individuals,
- Asymptomatic (A): Infected and infective but showing mild or no symptoms
- Symptomatic (I): Infected and infective but showing symptoms described in the literature,
- Quarantined (Q): Symptomatic that are not infective,
- Hospitalized (H) Symptomatic, not infective, who are being treated,
- Removed (R) People removed from the epidemic dynamics by recovering or passing away.

[2]The software is written in python 3.7, and is made public at `https://github.com/wlyra/covid19`

medRxiv preprint doi: https://doi.org/10.1101/2020.04.09.20060053; this version posted April 15, 2020. The copyright holder for this preprint (which was not certified by peer review) is the author/funder, who has granted medRxiv a license to display the preprint in perpetuity. It is made available under a CC-BY-NC-ND 4.0 International license .

We split that the population in subcategories by age (range, 0-10, 10-20, 20-30, 30-40, 40-50, 50-60, 60-70, 70-80, and 80+ years old) and that rates should vary with age [18].

Taking into consideration the 8 compartments and the 9 age groups, the model is described by a set of 72 coupled non-linear equations:

$$\frac{dS_i}{dt} = -\lambda(t)S_i - \psi_i(t)S_i + \phi_i(t)C_i, \tag{1}$$

$$\frac{dC_i}{dt} = \psi_i(t)S_i - \phi_i(t)C_i, \tag{2}$$

$$\frac{dE_i}{dt} = \lambda(t)S_i - \sigma E_i, \tag{3}$$

$$\frac{dA_i}{dt} = (1-p)\sigma E_i - \theta A_i, \tag{4}$$

$$\frac{dI_i}{dt} = p\sigma E_i - (\gamma+\xi)I_i + (1-w)\theta A, \tag{5}$$

$$\frac{dQ_i}{dt} = \gamma I_i - \xi Q_i, \tag{6}$$

$$\frac{dH_i}{dt} = q_i\xi I_i - \eta H_i, \tag{7}$$

$$\frac{dR_i}{dt} = w\theta A_i + (1-q_i)\xi I_i + \eta H_i. \tag{8}$$

For each compartment X the age sub-bins add up to $X = \sum_i X_i$ and compartments are such that $S + C + E + A + I + Q + H + R = N$, with $N = \sum_i N_i$ being the total population; N_i is the population in each age bin.

Eqs. (1)–(8) describe a compartmentalization of the population and the flow between the compartments. Contact with infected individuals removes a fraction of the susceptible (S) population at a rate given by λ, referred to as infection force, making them exposed (E) to (SARS-CoV-2) . Exposed (E) becomes infectious at the rate σ; a fraction p of them becoming symptomatic (I) and $(1-p)$ asymptomatic (A). The symptomatic (I) are removed from the infective force and become quarantined (Q)at a rate γ, the asymptomatic (A) are removed at a rate θ, a fraction w of them going in remission (a fraction $(1-w)$ becomes symptomatic. A fraction q_i of the quarantined (Q) are hospitalized at a rate ξ. The hospitalized (H) are removed at a rate η. The average fatality rate is μ_i.

The timescales corresponding to σ, γ, θ, ξ, and η are the incubation time $t_\sigma = \sigma^{-1}$ the infectious interval $t_\gamma = \gamma^{-1}$, the remission time $t_\theta = \theta^{-1}$, the time to hospitalization $t_\xi = \xi^{-1}$, and the average length of hospital stay $t_\eta = \eta^{-1}$.

The infection force is driven by the infected, both symptomatic (I) and asymptomatic (A)

$$\lambda(t) = \beta(t)\mathcal{I} \tag{9}$$

where we use the shorthand notation

$$\mathcal{I} = \sum_i \frac{(I_i + A_i)}{N_i} \tag{10}$$

and β is the infection rate, related to the reproduction number $\mathcal{R}(t)$ via

$$\mathcal{R}(t) = \frac{\beta(t)}{\gamma}. \tag{11}$$

Lock-down consists of having a fraction of the susceptible population removed from the epidemic dynamic by moving them from S_i to C_i at a rate ψ_i .Similarly, lifting the

medRxiv preprint doi: https://doi.org/10.1101/2020.04.09.20060053; this version posted April 15, 2020. The copyright holder for this preprint (which was not certified by peer review) is the author/funder, who has granted medRxiv a license to display the preprint in perpetuity. It is made available under a CC-BY-NC-ND 4.0 International license .

lock-down is done by placing C_i into S_i at the rate ϕ_i. We consider these functions to be Dirac deltas

$$\psi_i = a_i \; \delta(t - t_{\text{lock}}) \tag{12}$$

$$\phi_i = b_i \; \delta(t - t_{\text{lift}}) \tag{13}$$

where t_{lock} and t_{lift} are the time (in days) of lock-down and of lifting of the lock-down, respectively. To allow for partial demographic lock-downs (e.g., 80% lock-down of the population are in complete lock-down), a_i and b_i are allowed to vary by age (e.g., 80% lock-down of the 40's age group population are in complete lock-down). The flow chart between compartments is shown in Fig. 1.

Other diagnostic quantities are the numbers U_i of people in need of an intensive care unit (ICU) bed

$$U_i = \zeta_i H_i \tag{14}$$

where ζ_i is the fraction of hospitalized patients that need critical care. Both ζ_i and the hospitalization fraction q_i are age-stratified.

For integration, we use a standard Runge-Kutta algorithm, with timesteps

$$\Delta t = \frac{1}{2} \left[\max\left(\beta, \gamma, \theta, \sigma, \xi, \eta\right)\right]^{-1} \tag{15}$$

Model validation

In this section we present details about the model validation and strategies to verify characteristic timescales and other parameters.

Model fit to the 2020 COVID-19 epidemic

We consider the susceptible population (S) as the total population of a country since at the onset of outbreak no one is immune to the virus yet. Model parameters, shown in Table 1, were based on previous knowledge of Coronaviruses and early reports and research on COVID-19 [19]. The age-dependent parameters fatality rate μ_i, fraction of infectious that are hospitalized q_i, and fraction of hospitalized that need critical care are shown in Table 2.

Table 1. Priors of timescales and ratios for the MCMC modeling.

Parameter	Symbol	Value
Incubation time	σ^{-1}	5.2 days
Infectious interval	γ^{-1}	2.9 days
Symptomatic fraction	p	0.6
Remission time	θ^{-1}	14 days
Remission fraction of asymptomatic	w	0.8
Time to hospitalization	ξ^{-1}	5 days
Time at hospital	η^{-1}	10 days

Table notes: Values taken from [18].

Because all these timescales are much smaller than a human lifetime, aging of the population is ignored and no upward flow between the age sub-compartments

medRxiv preprint doi: https://doi.org/10.1101/2020.04.09.20060053; this version posted April 15, 2020. The copyright holder for this preprint (which was not certified by peer review) is the author/funder, who has granted medRxiv a license to display the preprint in perpetuity. It is made available under a CC-BY-NC-ND 4.0 International license .

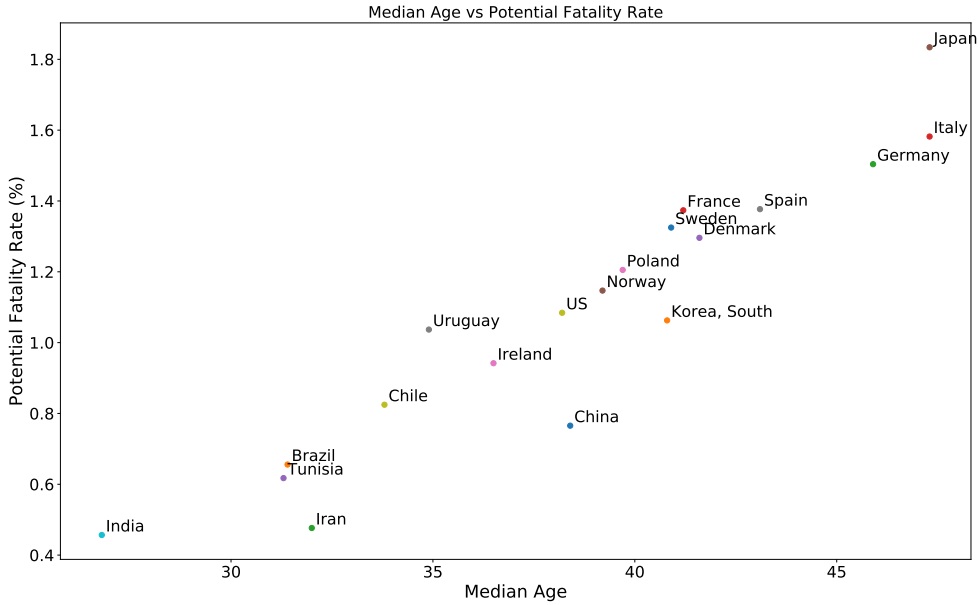

Fig 2. Fatality rate as a function of median age. The fatality rate by age bins is taken from [18] and the population pyramids from UN data.

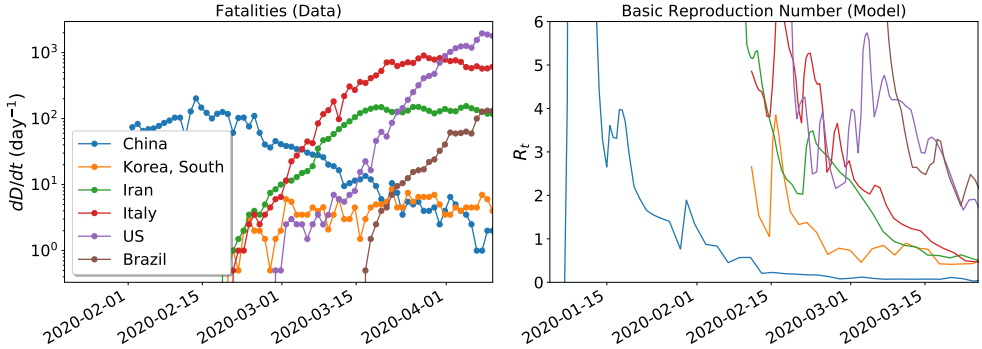

Fig 3. *Left*: The time series of fatalities for a number of countries. *Right*: the time derivative of the curve of fatalities is converted into $\mathcal{R}(t)$ according to Eq. (19).

medRxiv preprint doi: https://doi.org/10.1101/2020.04.09.20060053; this version posted April 15, 2020. The copyright holder for this preprint (which was not certified by peer review) is the author/funder, who has granted medRxiv a license to display the preprint in perpetuity. It is made available under a CC-BY-NC-ND 4.0 International license .

$(i \to i+1)$ is considered. Population pyramids are taken from UN data [3], and split into the pre-defined age bins.

We derive $\mathcal{R}(t)$ from the available statistics since knowledge on the real number of infected is not clear. The most reliable indicator in this situation is the number of deaths. Given a fatality rate μ and an average time τ between exposure and death, the number of dead at a time $t+\tau$ will equal the fatality rate times the number of people that got exposed at time t. Assuming that confinement dynamics do not play a role (although it is trivial to include it), the equation is the following:

$$\Delta D_i(t+\tau) = -\mu_i \Delta S_i(t). \tag{16}$$

Taking the continuous limit and substituting Eq. (1)

$$\frac{d}{dt} D_i(t_r) = \mu_i \lambda(t) S_i \tag{17}$$

where we also write $t_r = t+\tau$ for the retarded time. Summing over all age bins $D = \sum_i D_i$ we have the cumulative death rate on the LHS, which is an observable

$$\frac{d}{dt} D(t_r) = \lambda(t) \langle \mu S \rangle \tag{18}$$

and $\langle \mu S \rangle = \sum_i \mu_i S_i$. We can then substitute Eq. (9) and solve for $\mathcal{R}(t)$ as a function of time

$$\mathcal{R}(t) = \frac{1}{\gamma \mathcal{I} \langle \mu S \rangle} \frac{d}{dt} D(t_r). \tag{19}$$

Since death occurs an average of τ days after infections, we setup the integration to start τ days before the first reported COVID-19 death, i.e., $t=0$ means $t_r = \tau$. Finally, to start the integration we need to define the initial number of exposed individuals. This should be

$$E_0(t_0) = \overline{\mu}^{-1} D_0(t_0 + \tau) \tag{20}$$

where t_0 is the time of the first death and $\overline{\mu} = N^{-1} \sum_i \mu_i n_i$ is the age-weighted fatality rate. According to current knowledge of the epidemics, $\tau \approx 14$ days [18].

We compared our model predictions with official data on cases and deaths for multiple countries, as tracked by the Center for Systems Science and Engineering (CSSE) at Johns Hopkins University [4]. We plot in the left panel of Fig. 3 the fatality rate for a number of countries, which corresponds to the left hand side of Eq. (18). We apply Eq. (19) to convert this data into $\mathcal{R}(t)$, feeding this value into Eq. (1)-Eq. (8) to start the SEIR evolution. The populations $I(t)$ and $S(t)$ that enter in Eq. (19) are then calculated to update $\mathcal{R}(t)$. The resulting values are plotted in the right-hand-side of Fig. 3.

The timescales σ, γ, θ, and ξ, as well as the fractions p and w, are found by Markov chain Monte Carlo (MCMC) fitting, with priors as given in Table 1 and explained in the Supporting Information (Markov Chain Monte Carlo).

Finally, we compare the cumulative number of hospitalizations calculated from our model with the number of confirmed COVID-19 cases. For a country that is not doing massive testing and only reporting COVID-19 as acute cases reach the hospital, these curves should match reasonably well.

[3] https://www.populationpyramid.net

[4] `https://systems.jhu.edu/research/public-health/ncov/`

medRxiv preprint doi: https://doi.org/10.1101/2020.04.09.20060053; this version posted April 15, 2020. The copyright holder for this preprint (which was not certified by peer review) is the author/funder, who has granted medRxiv a license to display the preprint in perpetuity. It is made available under a CC-BY-NC-ND 4.0 International license .

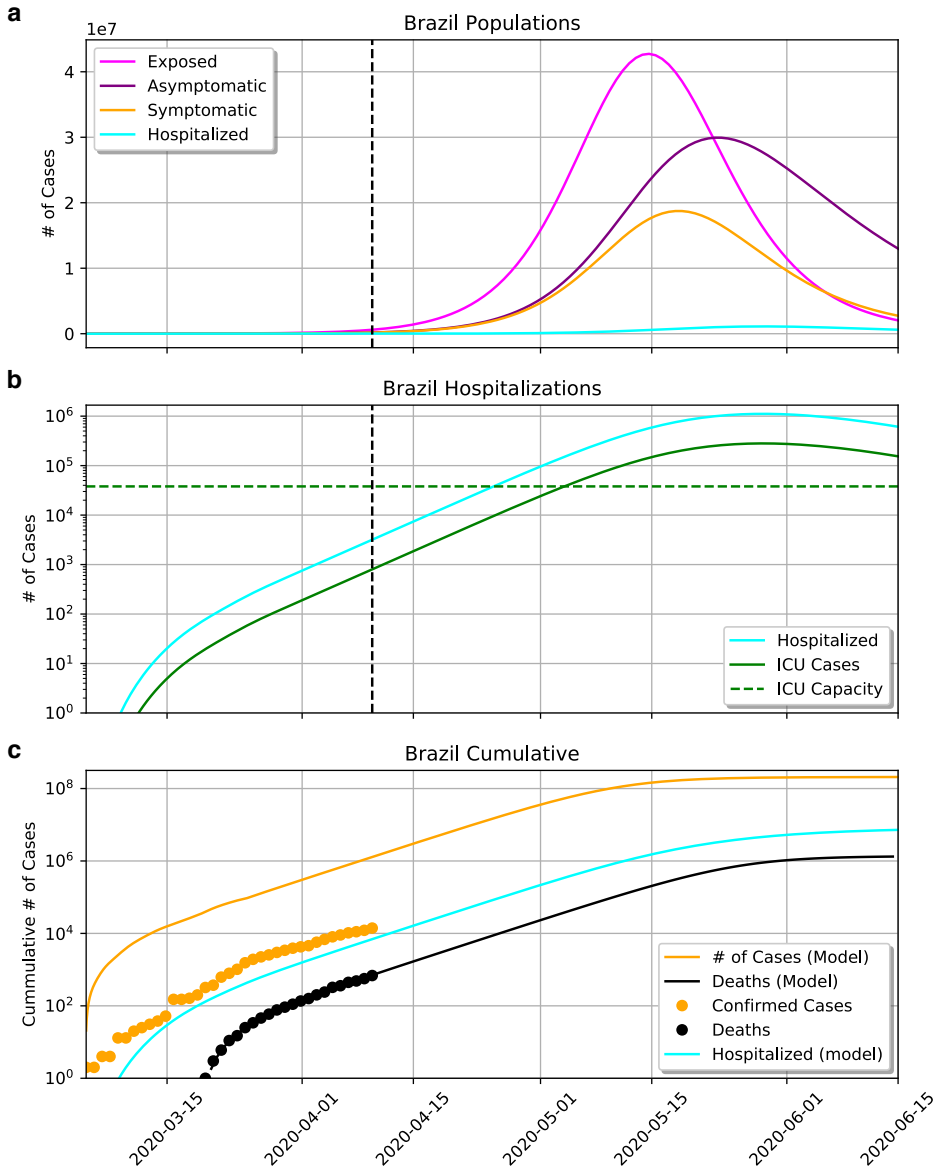

Fig 4. a) Evolution of the compartments of exposed (E), asymptomatic (A), symptomatic (I) and hospitalized (H). b) The same curve of H, and the fraction of hospitalizations needing ICU (U). The green dashed curve shows the total number of ICU beds in the country. At the current rate, the epidemics should peak in mid-May and collapse of the health care system by May 1st. c) cumulative number of reported cases and fatalities as orange and black dots, respectively. The number of hospitalizations closely matches the number of confirmed cases.

medRxiv preprint doi: https://doi.org/10.1101/2020.04.09.20060053; this version posted April 15, 2020. The copyright holder for this preprint (which was not certified by peer review) is the author/funder, who has granted medRxiv a license to display the preprint in perpetuity. It is made available under a CC-BY-NC-ND 4.0 International license .

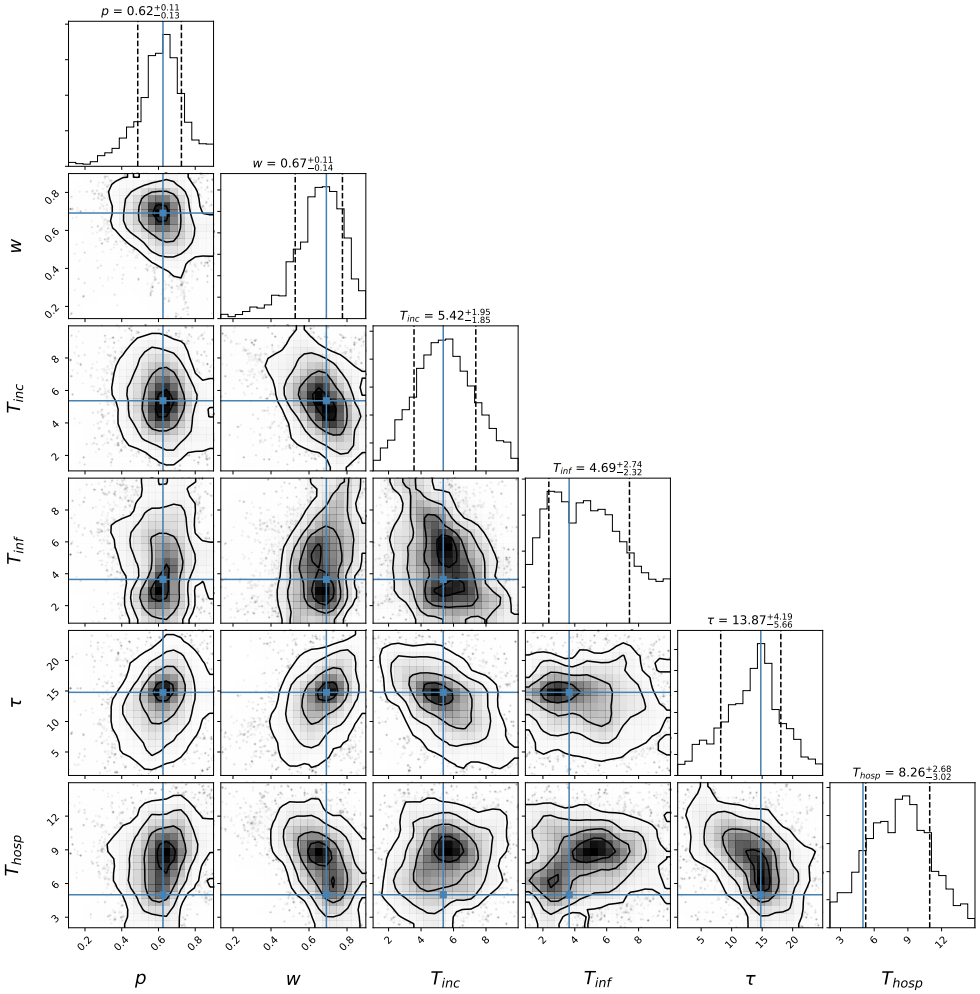

Fig 5. Posterior probabilities for the epidemic parameters determined by the MCMC modeling.

medRxiv preprint doi: https://doi.org/10.1101/2020.04.09.20060053; this version posted April 15, 2020. The copyright holder for this preprint (which was not certified by peer review) is the author/funder, who has granted medRxiv a license to display the preprint in perpetuity. It is made available under a CC-BY-NC-ND 4.0 International license .

Table 2. Age-dependent parameters.

Age bins	μ_i ($\times$100)	q_i ($\times$100)	ζ_i ($\times$100)
0-10	0.002	0.1	5
10-20	0.006	0.3	5
20-30	0.03	1.2	5
30-40	0.08	3.2	5
40-50	0.15	4.9	6.3
50-60	0.60	10.2	12.2
60-70	2.2	16.6	27.4
70-80	5.1	24.3	43.2
80+	9.3	27.3	70.9

Table notes: Values taken from [18].

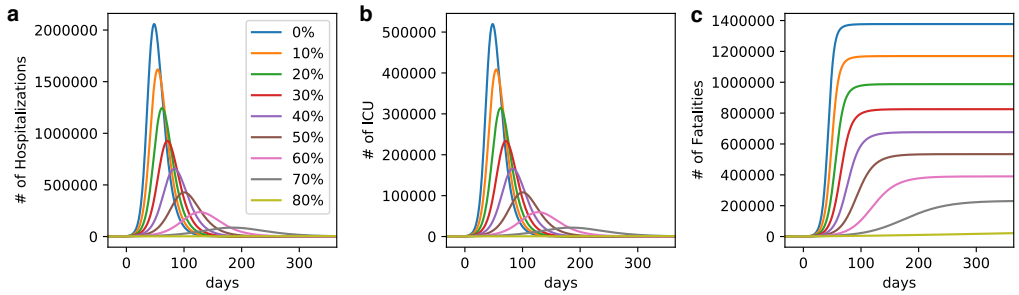

Fig 6. a) Number of hospitalizations. b) ICU cases. c) Fatalities. The three curves are as a function of the degree of horizontal confinement. To not overwhelm the health care system capacity ($\approx 3 \times 10^4$) ICU beds, the level of social distancing should be over 70%. Brazil is managing 56%.

Results and Discussion

Brazil epidemic scenario

Fig. 4 represents the modeled epidemic scenario in Brazil over 400 days time (checked a posteriori as the time when the number of symptomatic cases ends with a 70% horizontal lockdown). Parameters determined by the MCMC modeling are shown in Fig. 5, being $p = 0.62^{+0.11}_{-0.13}$, $w = 0.67^{0.11}_{-0.14}$, $T_{\text{inc}} = 5.42^{1.95}_{1.85}$, $T_{\text{inf}} = 4.69^{2.74}_{2.32}$, $T_{\text{remission}} = 13.87^{4.19}_{-5.66}$, and $T_{\text{hosp}} = 8.26^{2.68}_{-3.02}$. $\mathcal{R}(t)$ at present is hovering around 2.

Fig. 4a shows the evolution of the compartments of exposed (E), asymptomatic (A), symptomatic (I), and hospitalized (H), in linear scale. Fig. 4b shows the same curve of H but also the fraction of hospitalizations needing ICU (U), in log scale. The epidemic is starting at March 1st and number of symptomatic is predicted to end at July 1st. The peak of symptomatics is predicted for May 17th with 20 million symptomatics. Consequently, there is a predicted rise in number of hospitalized, reaching saturation on May 3rd and peaking at May 22nd with 10^6 hospitalized. ICU beds will reach saturation on May 3rd, when the ≈ 35 thousand ICU beds in Brazil are occupied (since the estimate assumes that all ICU beds should be occupied with coronavirus patients, which is not realistic, the collapse should in fact happen sooner). Demand for ICU will get higher until reaching a peak on May 22nd with 300 000 patients. The cumulative number of deaths June 1st is 10^6.

Fig. 4 contrasts the predicted cumulative numbers of infected persons (orange line), hospitalized persons (blue line), and deaths (black line). In this figure, the cumulative number of confirmed cases (yellow dots) and deaths (black dots). The cumulative

medRxiv preprint doi: https://doi.org/10.1101/2020.04.09.20060053; this version posted April 15, 2020. The copyright holder for this preprint (which was not certified by peer review) is the author/funder, who has granted medRxiv a license to display the preprint in perpetuity. It is made available under a CC-BY-NC-ND 4.0 International license .

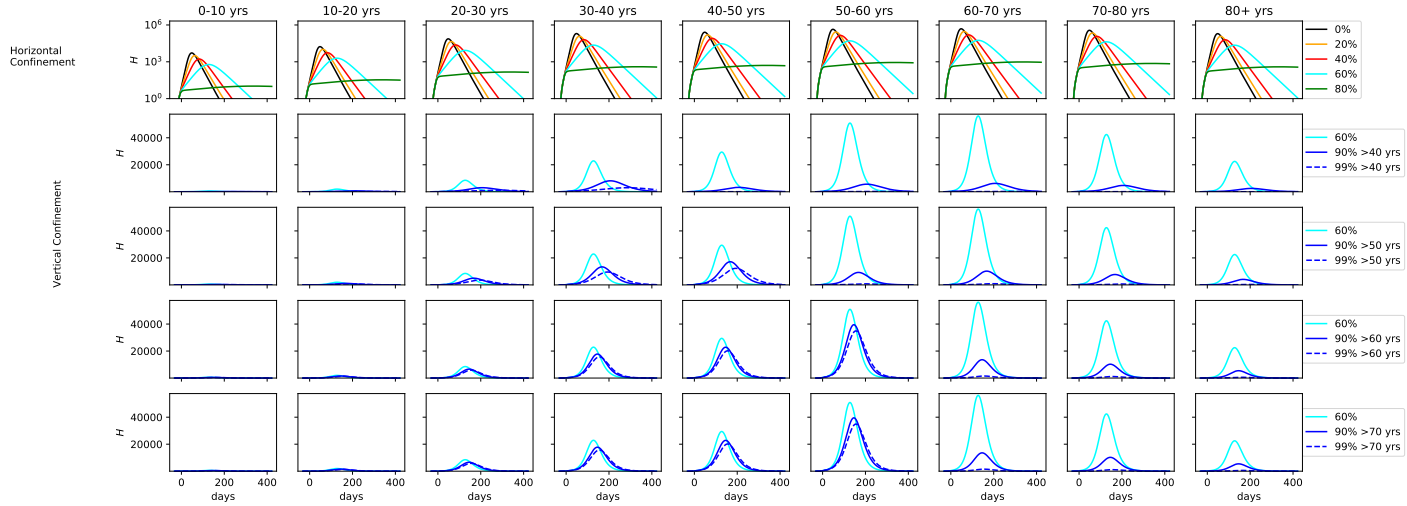

Fig 7. *Upper:* Number of hospitalizations in horizontal confinement with different proportions of the population, broken down by age. *2nd row:* 60% of the population under 40 is confined, the population older than 40 is confined to a higher degree, at 90% (solid blue line) and 99% (dashed blue line). The 3rd, 4th, and 5th row of plots show the same analysis but confining 60% up 50, 60, and 70 years old, respectively.

number of hospitalized is very close to the actual confirmed cases. This is expected as Brazil is not doing testing on a massive scale.

Horizontal Lockdown

In Fig. 6 we check the effect of horizontal confinement, defined as equal percentage of the population confined at any age bin. There is a change in the epidemic dynamic when horizontal confinement is applied in different rates Fig. 6 The plots show (a) the number of hospitalizations, (b) the number of ICU cases, and (c) the number of fatalities, as a function of the degree of social distancing. Confinement was implemented at time $t = 0$ corresponding to March 22 when the first measurement of social distancing was implemented. To not overwhelm the health care system capacity ($\approx 4 \times 10^4$) ICU beds, the level of social distancing should be over 70%. As mentioned in the introduction, estimates are that Brazil is maintaining 56% (with state to state variation from a maximum of 64.7% to a minimum of 53.7%) . At this low level of distancing, capacity should be reach in less than 50 days, which is in agreement with the dynamical $\mathcal{R}(t)$ model in Fig. 4.

Vertical Lockdown

We vary now the degree of confinement by age bin, characterizing the vertical confinement. Fig. 7 shows the number of hospitalizations in a model where confinement was implemented, broken down by age bins. The upper plots show horizontal confinement with different proportions of the population (same as Fig. 6 but broken down by age and in logarithmic scale). Confinement was implemented at the same time as in Fig. 6. The other rows explore vertical confinement. In the second column 60% of the population under 40 is confined, but the population older than 40 is confined to a higher degree, at 90% (solid blue line) and 99% (dashed blue line). The cyan line marks the same model as the upper plots, where 60% of the population is confined, irrespective

medRxiv preprint doi: https://doi.org/10.1101/2020.04.09.20060053; this version posted April 15, 2020. The copyright holder for this preprint (which was not certified by peer review) is the author/funder, who has granted medRxiv a license to display the preprint in perpetuity. It is made available under a CC-BY-NC-ND 4.0 International license .

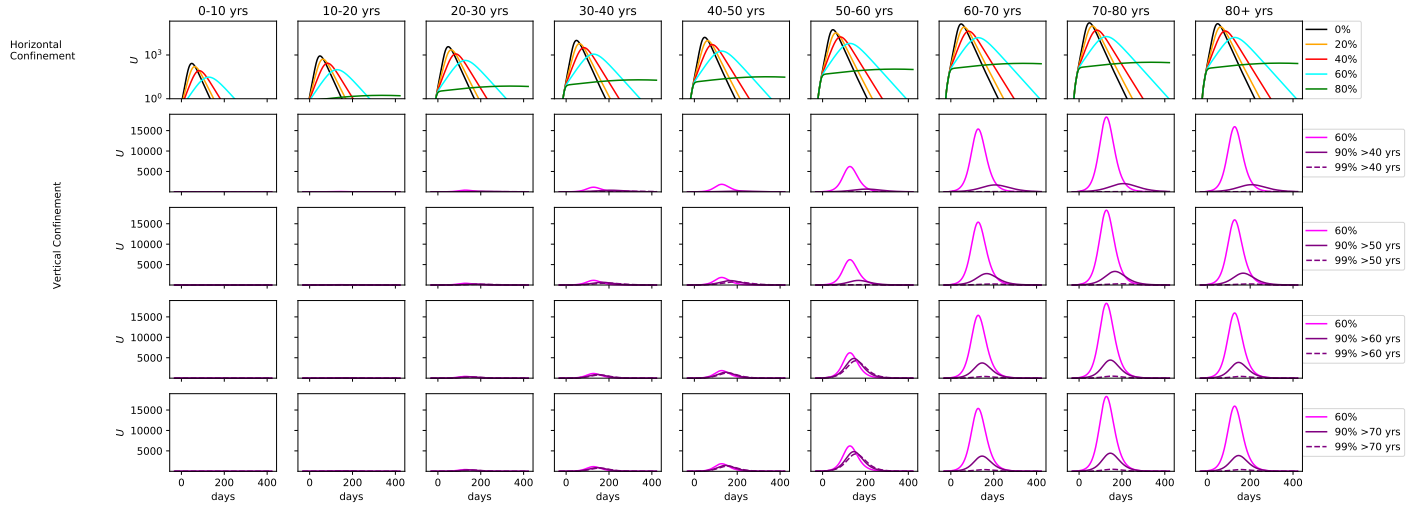

Fig 8. *Middle:* Same as Fig. 7, but for fraction of hospitalized that need ICU.

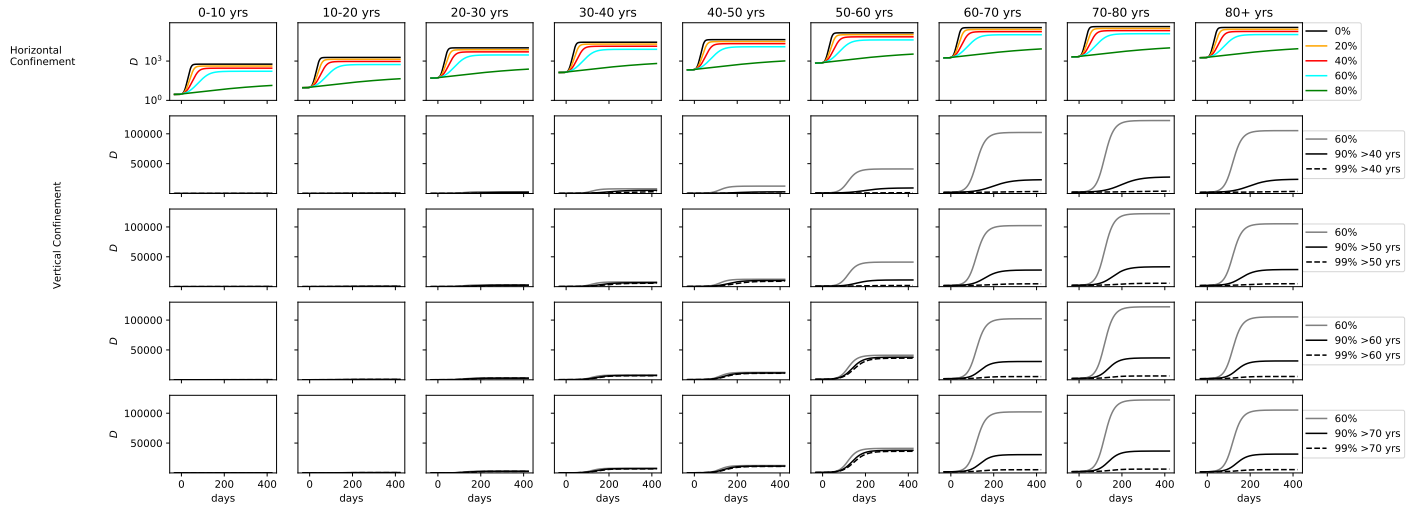

Fig 9. Same as Fig. 7, but for the number of fatalities.

medRxiv preprint doi: https://doi.org/10.1101/2020.04.09.20060053; this version posted April 15, 2020. The copyright holder for this preprint (which was not certified by peer review) is the author/funder, who has granted medRxiv a license to display the preprint in perpetuity. It is made available under a CC-BY-NC-ND 4.0 International license .

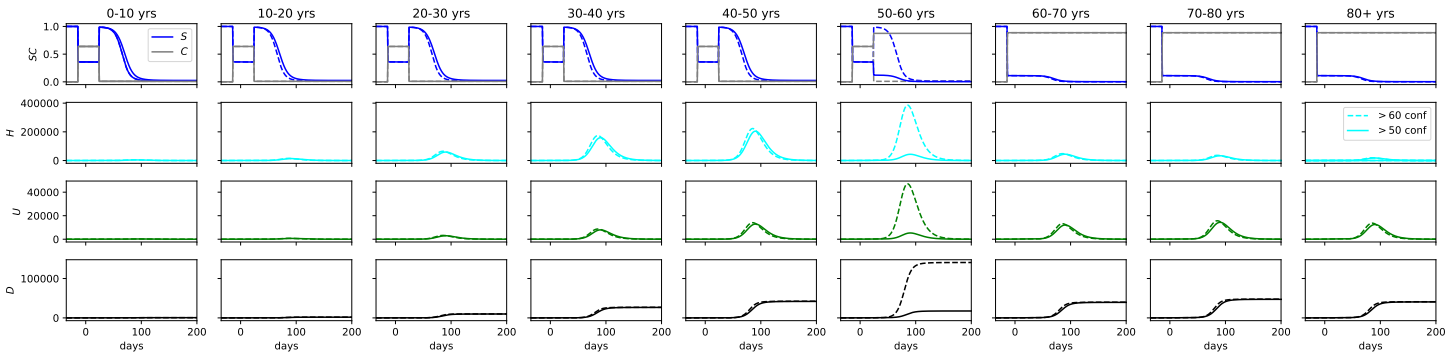

Fig 10. Vertical confinement as exit strategy after a horizontal lockdown of 60% was held, from March 22nd to May 1st. *Upper plots:* S and C compartments, normalized by the number of individuals in the respective age bin. *2nd row:* number of hospitalizations, *3rd row:* number of ICU cases, *lower plots:* cumulative number of fatalities. The figure shows full release for the population under 50 (dashed line) and under 60 (solid line). The population past this age is kept at 90% confinement.

of age. The 3rd, 4th, and 5th row of plots show the same analysis but confining 60% up 50, 60, and 70 years old, respectively. As seen in the cyan line, the number of hospitalized rises from 30-60 and falls for 70 onwards. That is because even though 70+ are more likely to be hospitalized, the number of 30-60 is much higher in the population.

Fig. 8 shows the same results for the fraction of hospitalized that needs ICU. Fig. 9 shows results from the same suite of models but for the number of fatalities. For the number of ICU cases, there is no significant difference past age 60, with only a minor uptick at the 70-80 age range. Collapse of health care system can be avoided if vertical confinement is instored on people who are 60 or older, but at the expense of a significant number of extra ICU cases for the 50-60 age bin. At 60% confinement, hundred of thousands of deaths are seen in the 60-70, 70-80, and 80+ age bins. The number lowers to 50 000 in the 90% confinement. As noted before, vertical confinement for 60 years old and older, leads to a significant number of deaths for the 50-60 age bin (over 50 000). Vertical confinement at 50 years old leads to much lower death rate for this age segment.

Finally, we look at vertical confinement as an exit strategy. In Fig. 10 we model a release from lockdown on May 1st, according to two scenarios: full release for the population under 50 (dashed line) and full release for the population under 60 (solid line). The population past this age is kept at 90% confinement. The upper plots show the susceptible (S) and confined compartments (C), normalized by the number of individuals in the respective age bin. The second row from top to bottom shows the number of hospitalizations, the third row the number of ICU cases, and the last row the cumulative number of fatalities. As the population is released from global confinement, the number of $H/U/D$ peaks at 400 000/50 000/120 000 in the 50-60 age bin alone, that bears the lion's share of morbidity. Keeping the 50-60 age population in 90% confinement lowers the statistics significantly, with the health care system at capacity, and the number of deaths per age bin about 25 000, with 60+ years olds having the same fatalities as 40-50 years old.

Limitations

As in any setting, the outbreak response strategy plays a crucial role in quality of the outputs models can give.Since the identification of first case, In Brazilian response strategy has been changing over time. At first, only international travelers admitted to hospitals had access to SARS-CoV-2 testing. Now there are diagnostic clinics and

medRxiv preprint doi: https://doi.org/10.1101/2020.04.09.20060053; this version posted April 15, 2020. The copyright holder for this preprint (which was not certified by peer review) is the author/funder, who has granted medRxiv a license to display the preprint in perpetuity. It is made available under a CC-BY-NC-ND 4.0 International license .

universities involved in COVID-19 testing, but there is no national massive testing strategy in place. Besides, each Brazilian state has the authority to put in place their own strategy to address the epidemic. The states of São Paulo and Rio de Janeiro, containing the largest metropoles in the country, adopted larger strategies of isolation with schools and stores closed early on while similar strategies had not yet been adopted in other states. Bottom line, the resulting morbidity and mortality rates can change significantly, resulting in dramatically different output numbers as the number of infected people or the number of hospital beds needed. It is necessary to have massive testing strategy in place to have better prediction accuracy of the models.

Our model estimate hundreds of thousands of infected people in Brazil at April 1st. This is more than the number of expected cases in the country while we write this article, considering the estimated under notification of cases [20] and do nothing to control the infection. It is possible that the actual number be less than that although it is also important to notice Brazil has not done a real lockdown so far.

The model also ignores mobility, in the sense that it does consider travel to and from the country. Given that right now we are the stage of community transmission, this limitation should not be of significance to the results.

Conversely, and more importantly, the model assumes that the confined population is completely safe from infection, whereas in reality a vertical lockdown may not be feasible to implement as the elderly are not adequately distanced from the younger in their family and/or social circle, and infection cannot be avoided if the younger is exposed to COVID-19 .

Finally, the analysis assumes that the data on fatalities is accurate. Underreported deaths should lead to an unknown source of error in the present study. Also, the MCMC produces error bars in the parameters that we did not take into account in the forward modeling.

Conclusion

Is this study we examine the strategy of vertical confinement as currently debated in Brazil.

Since the fatality rate of COVID-19 appears to be higher among the elderly population, we studied how confinement of age bins (particularly 60 and beyond) affect the demand for hospital beds and intensive care beds.

Our model suggests that at the current rate of advance of the pandemics, Brazil should face collapse of the health care system by May 15th, with 300 000 ICU beds needed (10 times more than the current capacity), and 10^6 fatalities. A decrease in the rate of confirmed cases is seen with respect to the rate of fatalities, which is indicative of the effect of the lockdown. A 60% lockdown reduces the number of deaths to 400 000 due to COVID-19, still not avoiding overload of the health care system. An increase in lockdown to 70% is needed to avoid the number of cases overcome the number of available critical care beds.

An exit strategy of confinement of individuals older than 60 years old by May 1st would see a second wave disproportionally affect the 50-60 age bin. The ICU cases in this age range alone would bring the health care system to collapse and result in over 100 000 deaths. Confinement by age group should consider the population over 50 years old as well. However, the age range 50-60yrs is also a part of the workforce, and thus defeats the purpose of a confinement by age. Moreover, we emphasize that our model assumes an idealized lockdown where the confined are perfectly insulated from contamination, while in reality there would be several practical barriers to it as the confined elderly would depend on the young for most essential activities, and a perfect lockdown would not be achieved in a multi-generational household, especially in close

medRxiv preprint doi: https://doi.org/10.1101/2020.04.09.20060053; this version posted April 15, 2020. The copyright holder for this preprint (which was not certified by peer review) is the author/funder, who has granted medRxiv a license to display the preprint in perpetuity. It is made available under a CC-BY-NC-ND 4.0 International license .

quarters such as found in the low and even middle income neighborhoods common in Brazil. Our results therefore discourage confinement by age as the only exit strategy. We urge Brazilian authorities to take action to prevent virus dissemination in the critical coming weeks.

Supporting information

Markov Chain Monte Carlo. To fit the best value to w and p, and to better constrain σ^{-1}, γ^{-1}, θ^{-1}, ξ^{-1}, we use the affine-invariant ensemble sampler for Markov chain Monte Carlo (MCMC) [21] to sample the parameter space around the solutions and evaluation of the parameter uncertainties. For the priors input, we use the values taken from the [18]. To search for the minimization of cumulative hospitalization H_{c}, we generated a cumulative error C_{err} on the reported confirmed cases C_c.

As the JHU-CSSE reports on the confirmed cases are given daily with some fluctuations, we need to take this into account while weighing all solutions by adding a 1-day error matrix together with the confirmed cases (being conservative). In an ideal scenario, the cumulative number of hospitalization would be the same as the number of confirmed cases. In real life, not all confirmed cases are hospitalized so we do not expect to fit the H_{c} with C_c. Rather, we weigh the C_c array with the H_{c} array using:

$$w_t = \frac{\sum C_c - H_{\mathrm{c}}}{n} \tag{21}$$

$$H'_c = H_{\mathrm{c}} + w_t \tag{22}$$

H'_c is the weighed cumulative hospitalizations and n is the length of the data. Following we get the residual between C_c and H'_c, and we used the negative binomial distribution to calculate each likelihood [22]:

$$\mathrm{Res} = C_c - H'_c \tag{23}$$

$$Z = \frac{\sum \frac{\mathrm{Res}}{C^2_{\mathrm{err}}}}{\sum \frac{1}{C^2_{\mathrm{err}}}} \tag{24}$$

$$P = \sum \frac{(\mathrm{Res} - Z)^2}{C^2_{\mathrm{err}}} \tag{25}$$

$$P' = -0.5P \tag{26}$$

Equations 21 to 26 are implemented in the likelihood function on the code. If in each run it returns a finite number, the algorithm parses the result, if not it returns a large number (10^{20}) to discard as a bad fit.

We limit each parameter using a range cutoff in when feeding the probability function to restrict parameter space. That way, we do not run models with unrealistic physical parameters (such as e.g. symptomatic going to the hospital in -2 days), and also constrain the known range for the other parameters. The MCMC function feeds on 6 free parameters, 4 fixed parameters and 2 predetermined arrays as presented in Table 3.

References

1. WHO. Coronavirus disease 2019 (COVID-19) Situation Report - 75. World Health Organization; 2020. Available from: `https:`

medRxiv preprint doi: https://doi.org/10.1101/2020.04.09.20060053; this version posted April 15, 2020. The copyright holder for this preprint (which was not certified by peer review) is the author/funder, who has granted medRxiv a license to display the preprint in perpetuity. It is made available under a CC-BY-NC-ND 4.0 International license .

Table 3. Input parameters and arrays for MCMC

Parameter	Type	Value
T_{inc}: Incubation time	free	1 - 10 days
T_{inf}: Time while Infectious	free	1 - 5 days
p: Symptomatic fraction	free	0.2 - 1.0
τ: Days to remission after the infection	free	6 - 20 days
w: Remission fraction of asymptomatic	free	0.2 - 1.0
T_{hosp}: Time to hospitalization	free	5 days
Lockdown: date of the lockdown	fixed	date
release: date of the release of the lockdown	fixed	date
fatality rate age	fixed	array
T_{hosp2}: Days at hospital	fixed	10 days
q: hospitalization fraction age	fixed	array

Table notes: Priors taken from [18].

//www.who.int/docs/default-source/coronaviruse/situation-reports/20200404-sitrep-75-covid-19.pdf?sfvrsn=99251b2b{_}2.

2. Wu Z, McGoogan JM. Characteristics of and Important Lessons From the Coronavirus Disease 2019 (COVID-19) Outbreak in China: Summary of a Report of 72314 Cases From the Chinese Center for Disease Control and Prevention. JAMA. 2020;323(13):1239–1242. doi:10.1001/jama.2020.2648.

3. Bedford J, Enria D, Giesecke J, Heymann DL, Ihekweazu C, Kobinger G, et al. COVID-19: towards controlling of a pandemic. The Lancet. 2020;395(10229):1015–1018. doi:10.1016/S0140-6736(20)30673-5.

4. Buseh AG, Stevens PE, Bromberg M, Kelber ST. The Ebola epidemic in West Africa: Challenges, opportunities, and policy priority areas. Nursing Outlook. 2015;63(1):30 – 40. doi:https://doi.org/10.1016/j.outlook.2014.12.013.

5. Gates B. The Next Epidemic - Lessons from Ebola. New England Journal of Medicine. 2015;372(15):1381–1384. doi:10.1056/NEJMp1502918.

6. Oshitani H, Kamigaki T, Suzuki A. Major issues and challenges of influenza pandemic preparedness in developing countries. Emerging infectious diseases. 2008;14(6):875–880. doi:10.3201/eid1406.070839.

7. Remuzzi A, Remuzzi G. COVID-19 and Italy: what next? The Lancet. 2020;395(10231):1225 – 1228. doi:https://doi.org/10.1016/S0140-6736(20)30627-9.

8. WHO. Coronavirus disease 2019 (COVID-19) Situation Report - 79. World Health Organization; 2020. Available from: https://www.who.int/docs/default-source/coronaviruse/situation-reports/20200408-sitrep-79-covid-19.pdf?sfvrsn=4796b143{_}6.

9. WHO. Coronavirus disease 2019 (COVID-19) Situation Report - 72. World Health Organization; 2020. Available from: https://www.who.int/docs/default-source/coronaviruse/situation-reports/20200404-sitrep-75-covid-19.pdf?sfvrsn=99251b2b{_}2.

10. Chretien JP, Riley S, George DB. Mathematical modeling of the West Africa Ebola epidemic. eLife. 2015;4:e09186. doi:10.7554/eLife.09186.

medRxiv preprint doi: https://doi.org/10.1101/2020.04.09.20060053; this version posted April 15, 2020. The copyright holder for this preprint (which was not certified by peer review) is the author/funder, who has granted medRxiv a license to display the preprint in perpetuity. It is made available under a CC-BY-NC-ND 4.0 International license .

11. el Alami Laaroussi A, Ghazzali R, Rachik M, Benrhila S. Modeling the spatiotemporal transmission of Ebola disease and optimal control: a regional approach. International Journal of Dynamics and Control. 2019;7. doi:10.1007/s40435-019-00525-w.

12. Kuddus MA, Rahman A, Talukder M, Hoque A. A Modified Sir Model to Study on Physical Behaviour among Smallpox Infective Population in Bangladesh. American Journal of Mathematics and Statistics. 2014;2014:231–239. doi:10.5923/j.ajms.20140405.04.

13. Vargas-De-Leon C. Modeling control strategies for influenza A H1N1 epidemics: SIR models. Revista Mexicana de Fisica S. 2012;58:37–43.

14. Huang CY, Sun CT, Hsieh Jl, Lin H. Simulating SARS: Small-World Epidemiological Modeling and Public Health Policy Assessments. Journal of Artificial Societies and Social Simulation. 2004;7.

15. Kermack WO, McKendrick AG. A Contribution to the Mathematical Theory of Epidemics. Proceedings of the Royal Society of London Series A, Containing Papers of a Mathematical and Physical Character. 1927;115(772):700–721.

16. Kribs-Zaleta CM, Velasco-Hernández JX. A simple vaccination model with multiple endemic states. Mathematical Biosciences. 2000;164(2):183 – 201. doi:https://doi.org/10.1016/S0025-5564(00)00003-1.

17. DATASUS. Cadastro Nacional do Estabelecimentos de Saúde; 2019. Available from: `ftp://ftp.datasus.gov.br/dissemin/publicos/cnes/200508_/dados/LT`.

18. Ferguson N, Laydon D, Nedjati Gilani G, Imai N, Ainslie K, Baguelin M, et al. Impact of non-pharmaceutical interventions (NPIs) to reduce COVID19 mortality and healthcare demand. Published Online. 2020; p. 1–20. doi:10.25561/77482.

19. Kucharski A, Russell T, Diamond C, Liu Y, Edmunds J, Funk S, et al. Early dynamics of transmission and control of COVID-19: a mathematical modelling study. The Lancet Infectious Diseases. 2020;doi:10.1016/S1473-3099(20)30144-4.

20. Li R, Pei S, Chen B, Song Y, Zhang T, Yang W, et al. Substantial undocumented infection facilitates the rapid dissemination of novel coronavirus (SARS-CoV2). Science. 2020;doi:10.1126/science.abb3221.

21. Foreman-Mackey D, Hogg DW, Lang D, Goodman J. emcee: The MCMC Hammer. PASP. 2013;125(925):306. doi:10.1086/670067.

22. Gelman A, Carlin JB, Stern HS, Rubin DB. Bayesian Data Analysis. 2nd ed. Chapman and Hall/CRC; 2004.